Spatially averaged time-resolved particle-tracking velocimetry in microspace considering Brownian motion of submicron fluorescent particles

Y. Sato, S. Inaba, K. Hishida, M. Maeda

Abstract A time-series measurement method is proposed to detect velocity fields in a microchannel taking into account Brownian motion of submicron tracer particles. The present study proposes spatially averaged time-resolved particle-tracking velocimetry (SAT–PTV), which can detect temporal variations of fluid flow and eliminate errors associated with Brownian motion without losing temporal resolution. Velocity vectors of tracer particles obtained by PTV are spatially averaged in each interrogation window of particle-image velocimetry, yielding full velocity field information with temporal resolution. Synthetic particle images, which include Brownian motion of submicron fluorescent particles in flow fields with linear velocity gradients, are generated to validate the ability of SAT–PTV to track particles. SAT–PTV correctly captures the velocity gradient profiles. The spatial resolution based on the size of the first interrogation window and the measurement depth of the microscope system is 6.7 μm×6.7 μm×1.9 μm, within which several vectors are averaged. SAT–PTV is shown to measure the velocity field of a pulsating flow generated by an electrokinetic pump.

1
Introduction

Recent progress in micro- and nanotechnologies has yielded microfluidic devices that comprise microchannel networks for chip-based biological analyses handling small fluid sample volumes. For further development of microfluidic devices, e.g., lab-on-a-chip and micro total analytical systems (micro-TAS), quantitative measurements of microchannel flow are crucial to understand the physics of

Y. Sato (✉), S. Inaba, K. Hishida, M. Maeda
Department of System Design Engineering,
Faculty of Science and Technology, Keio University, 3-14-1 Hiyoshi,
Kohoku-ku, Yokohama 223-8522, Japan
E-mail: yohei@sd.keio.ac.jp
Fax: +81-45-5661720

transport processes in microspace. Experimental efforts by Brody et al. (1996) and Lanzillotto et al. (1997) contributed to the development of microspace flow measurements prior to the application of particle-image velocimetry (PIV), a well-established technique for macroscopic flow (Adrian 1991), in a microchannel to measure velocity fields.

Santiago et al. (1998) in their pioneering study of micron-resolution particle-image velocimetry (micro-PIV) measured velocity vectors in a Hele–Shaw flow with a spatial resolution of 6.9 μm×6.9 μm×1.5 μm, based on the size of the first interrogation window and depth-of-field of the objective lens. In this study, 300-nm diameter fluorescent particles were used as flow tracers, which include measurement errors associated with Brownian motion. Brownian motion effects on velocity detection were reduced by ensemble averaging. Meinhart et al. (1999) developed the micro-PIV technique using a pulsed Nd:YAG laser as the illumination source to measure velocity fields on the order of 1 mm s^{-1} in a microchannel with a spatial resolution of 13.6 μm×0.9 μm×1.8 μm. They showed accurate velocity profiles with time-averaged correlation functions (Meinhart et al. 2000b).

It can be seen that micro-PIV is a powerful tool for measuring microchannel flows. However, most transport processes in lab-on-a-chip and micro-TAS applications are unsteady phenomena. For temporal changes in velocity fields, it is hard to distinguish temporal variations of fluid flow from velocity fluctuations associated with Brownian motion using micro-PIV. Time-series measurement techniques are expected to contribute to the development of the assay process. From a viewpoint of microspace temperature measurements, Sato et al. (2003) accomplished a two-dimensional measurement technique in time series utilizing a fluorescent dye whose fluorescent intensity is strongly dependent on temperature. A novel time-series velocity measurement technique combined with the temperature diagnostic developed by Sato et al. (2003) is critical to the investigation of thermofluid dynamics in microspace.

The objective of the present study is to propose a spatially averaged time-resolved particle-tracking velocimetry (SAT–PTV) method in order to overcome these difficulties without losing temporal resolution. SAT–PTV eliminates Brownian motion effects on velocity vector detection, averaging PTV vectors within each interrogation window of PIV, i.e., calculating the mean displacement of tracer particles in each interrogation window, because Brownian motion is spatially random and unbiased. Validation of the capability of SAT–PTV is performed with synthetic particle images considering Brownian motion of
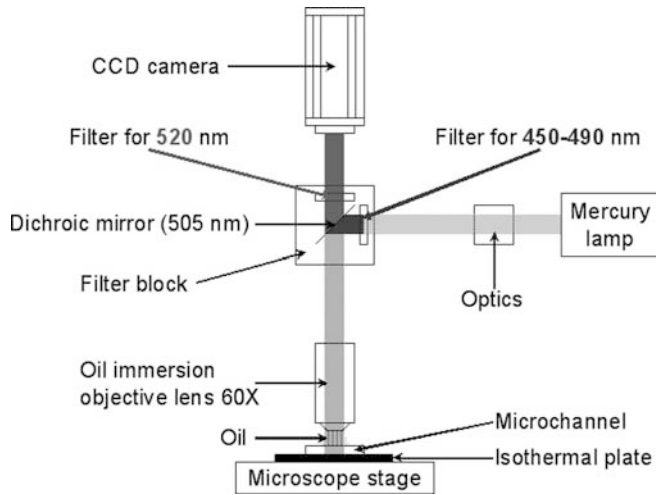
Fig. 1. Schematic of the measurement system

submicron fluorescent particles in flow fields with linear velocity gradients. The SAT–PTV method is applied to a pulsating flow generated by an electrokinetic pump. Important conclusions obtained in the present study enable us to utilize microspace transport phenomena, which are not yet fully understood, for the next generation of microfluidic devices.

2
Experimental apparatus

2.1
Optical measurement system
A schematic of the present optical measurement system is given in Fig. 1. A 12-bit cooled CCD camera (Hamamatsu Photonics, C4880-80) with a 656×494 array was mounted on a microscope (Nikon, E800). Illumination was provided by a continuous mercury lamp, which was then routed through a bandpass filter (450–490 nm) and a dichroic mirror transmitting wavelengths above 505 nm onto the microchannel. Fluorescence from the submicron particles were collected through a 60× magnification, oil-immersion objective lens (Nikon) with a numerical aperture of 1.4 and an emission filter transmitting wavelengths longer than 520 nm onto the CCD pixel sheet. The size of the CCD pixel sheet along with the objective lens used in the present study corresponded to a measurement area of 109 μm×82.3 μm in the object plane. The exposure time and frame interval of the CCD camera were 5.72 ms and 37 ms, respectively. Images were captured with a frame grabber (Coreco, IC-PIC) for further postprocessing and analysis. A thermally controlled stage maintained a constant temperature of 293 K to remove temperature effects on measurement results.

2.2
Submicron tracer particles
Properties of tracer particles (Duke Scientific) used for the reported experiments are compiled in Table 1. Submicron diameter particles are selected to achieve high spatial resolution and not disturb the flow field. Fluorescent

Table 1. Properties of fluorescent particles

Number mean diameter (nm)	200	400	1,000
Standard deviation of diameter (%)	<10	<5	<5
Density (g/cm^3)	1.05	–	–
Absorption wavelength (nm)	468	–	–
Emission wavelength (nm)	508	–	–
Measurement depth* (μm)	1.8	1.9	4.5

* The measurement depth was calculated from the equation given by Meinhart et al. (2000a) in which $n = 1.515$, $\lambda = 508$ and $NA = 1.4$.

particles are chosen to remove scattered light from the walls and substrate, which is a much bigger problem in microfluidic devices where the surface-to-volume-ratios are very high. The fluorescent particles allow selective acquisition of signal, which is important for the signal-to-noise ratio. The measurement depth was calculated from the equation given by Meinhart et al. (2000a)

$$\Delta z = \frac{3n\lambda}{NA^2} + \frac{2.16 d_{\mathrm{p}}}{\tan \theta} + d_{\mathrm{p}}, \qquad (1)$$

where n is the refractive index of the fluid between the objective lens and the microchannel, λ is the wavelength of light, NA is the numerical aperture of the objective lens and d_{p} is the diameter of tracer particles. For the experiments reported in Sect. 4, 400-nm diameter fluorescent particles were used as flow tracers.

2.3
Microchannels
Photolithography was used to fabricate the microchannels for the current experiments. A schematic of the microchannel is shown in Fig. 2. Photoresist (Micro-Chem, SU-8) was coated on a circular cover glass slide with a spin coater, yielding a thickness of 45 μm. The cover glass slide was baked in an oven at 373 K for 25 min and exposed with a mask under ultraviolet (UV) light for 40 s. The glass was further baked in the oven at 343 K for 15 min and was then soaked in a developer solvent for 5 min to lift off unexposed regions. In order to close the microchannel, SU-8 (used here as an adhesive material) was coated on a second cover glass slide with two 1-mm diameter holes, serving as an inlet and an outlet, by the spin coater to a thickness of 1 μm. The two cover glass slides were then placed together, baked at 373 K for 5 min in the oven, exposed to UV light for 2 min to harden and baked again at 373 K for 15 min. Deionized (DI) water seeded with submicron fluorescent particles was injected into the inlet and was pressure driven by a height difference established between the inlet and outlet fluid reservoirs. A channel Reynolds number, based on a channel width of 100 μm and a centerline mean velocity of 52.9 μm s^{-1}, is 6.17×10^{-3}.

3
SAT–PTV method

3.1
Effect of Brownian motion on velocity detection
When submicron particles are injected to track slow flows, errors caused by particle diffusion resulting from
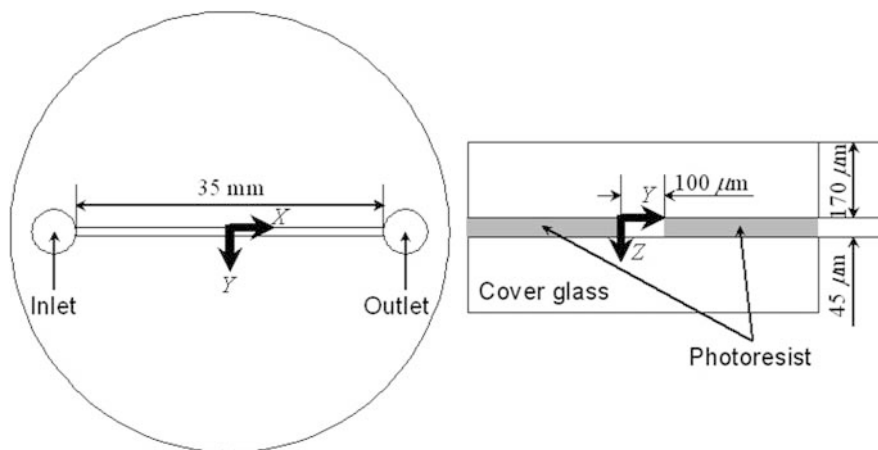
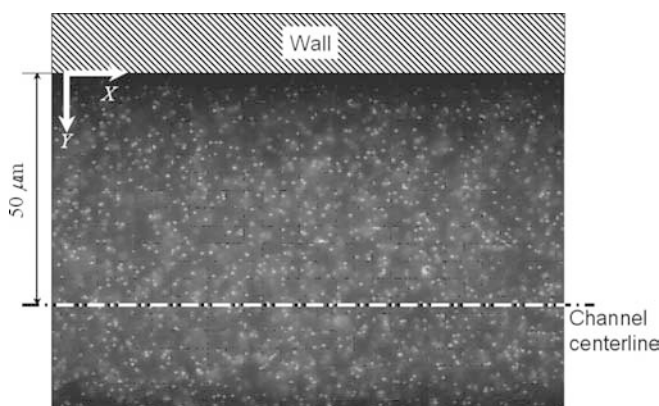Fig. 2. **a** Top and **b** cross-sectional views of the microchannel

Fig. 3. Instantaneous image of the steady flow in the microchannel containing 400-nm diameter fluorescent particles

Fig. 4. Instantaneous vector map in the microchannel at the Reynolds number of 6.17×10^{-3}
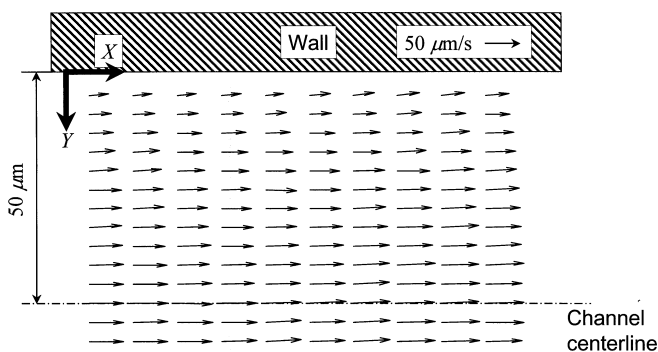
Fig. 5. Time-averaged vector map in the microchannel at the Reynolds number of 6.17×10^{-3}

Brownian motion are never neglected. An example was demonstrated by using 400-nm diameter fluorescent particles and the microchannel illustrated in Fig. 2. Figure 3 depicts a particle image at $z = 22.5$ μm, i.e., the depth-wise midpoint, in a steady flow captured by the present optical system. An instantaneous velocity vector field was obtained by PIV (Fig. 4). However, a noisy vector field is obtained for the laminar flow field as expected. The noise in the measured signal (velocity vectors) as shown in Fig. 4 is due to the influence of Brownian motion. Since Brownian motion is statistically random and is unbiased spatially and temporally, spatial and time-averaging substantially reduces Brownian noise. Figure 5 shows an ensemble average of ten instantaneous velocity field measurements calculated on a point-by-point basis. The effect of Brownian motion of tracer particles is eliminated by ensemble-averaging, and a high spatial resolution is achieved with micro-PIV (Meinhart et al. 1999).

The influence of Brownian motion on PIV should be considered in microflow: (1) when a distribution pattern of tracer particles in the interrogation window is changed due to Brownian motion for two successive images, spatial correlation always induces the measurement error. (2) For low velocities, if the root-mean-square of particle displacement associated with Brownian motion is comparable to the particle displacement for two successive images, it is hard to obtain velocity vectors by spatial correlation.
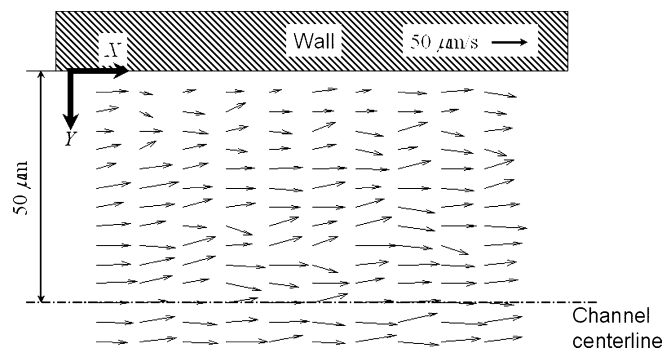
The dominant flow pattern in electrophoresis DNA chips or biochips is, however, unsteady flow such as accelerating flow or pulsating flow, therefore the micro-PIV technique eliminates not only velocity fluctuations associated with Brownian motion of tracer particles but also velocity variations of fluid flow that yield losses in temporal resolution. A new measurement method is necessary that is capable of measuring temporal variations of the flow field with Brownian motion of tracer particles included.

3.2
Overview of the method
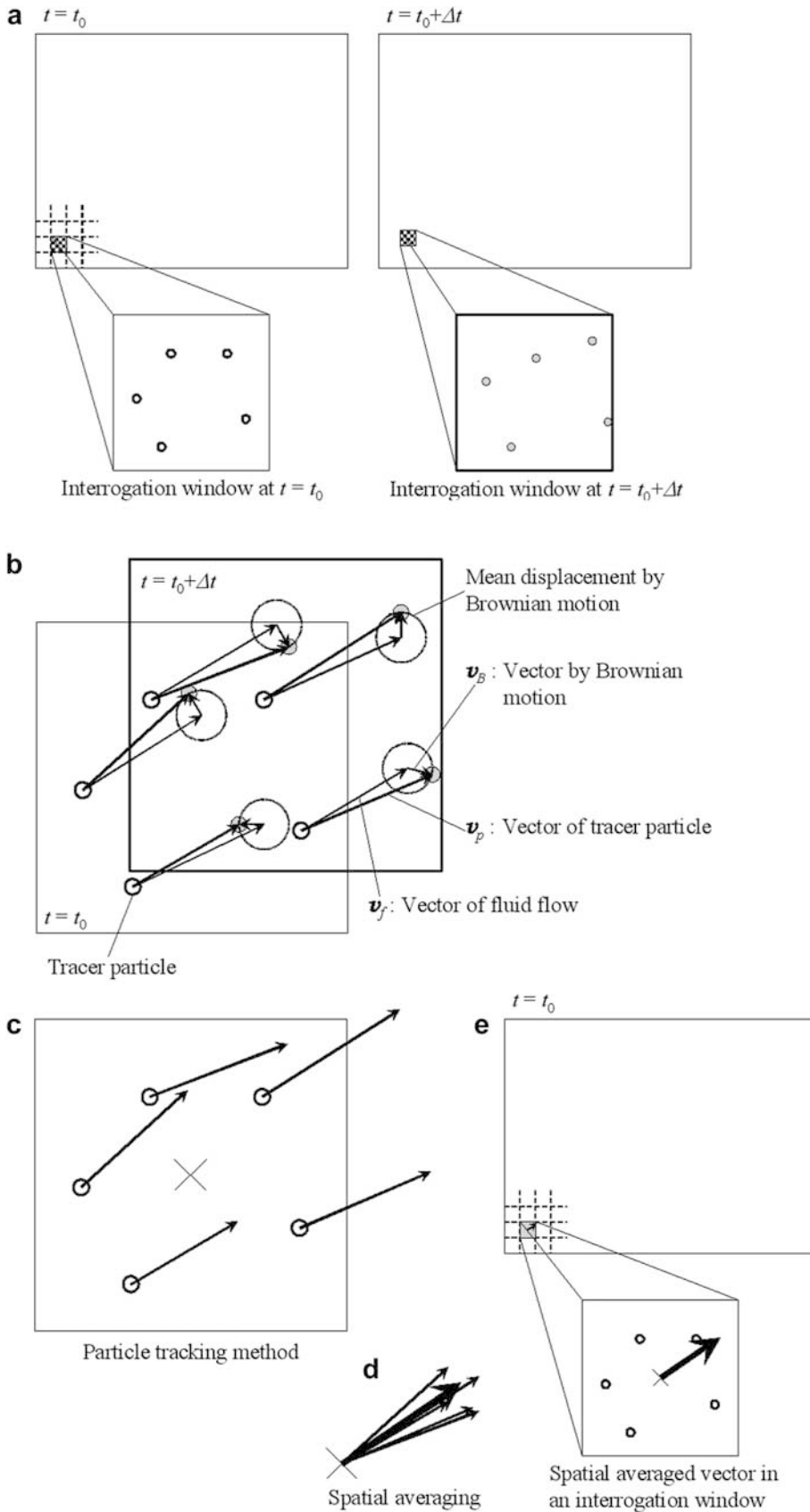A spatially averaged time-resolved particle tracking velocimetry (SAT–PTV) method is proposed to be applicable for

a $t = t_0$ $t = t_0 + \Delta t$

Interrogation window at $t = t_0$ Interrogation window at $t = t_0 + \Delta t$

b $t = t_0 + \Delta t$

Mean displacement by Brownian motion

$\boldsymbol{v}_B$: Vector by Brownian motion

$\boldsymbol{v}_p$: Vector of tracer particle

$\boldsymbol{v}_f$: Vector of fluid flow

$t = t_0$

Tracer particle

c

Particle tracking method

d

Spatial averaging

e $t = t_0$

Spatial averaged vector in an interrogation window

Fig. 6. Schematic of the SAT–PTV method considering Brownian motion effects on velocity vector detection

unsteady flows, since Brownian motion is spatially random and unbiased. When the flow direction of tracer particles is initially interrogated like super-resolution PIV (Keane et al. 1995), it is easy to pair individual particles at two successive images and the distance between particles is always larger than particle diffusion resulting from Brownian

motion. Based upon this idea, the SAT–PTV method can eliminate the effect of Brownian motion on velocity detection by averaging PTV vectors in each interrogation window of PIV without losing temporal resolution.

Figure 6 shows a schematic of the SAT–PTV method. A dynamic threshold binarization was implemented to extract each particle, and the centroid of the particle was determined using a Gaussain peak-fit method. A vector of the particle displacement obtained by PTV (Fig. 6b) v_p is comprised of a vector of a fluid flow v_f and a vector accounting for Brownian motion v_B at two successive images (Fig. 6a). When N particles are contained in an interrogation window (Fig. 6c) where spatial averaging is performed, the SAT–PTV vector is expressed as follows:

$$\frac{1}{N}\sum_{\text{window}} v_p = \frac{1}{N}\sum_{\text{window}} v_f + \frac{1}{N}\sum_{\text{window}} v_B. \qquad (2)$$

As Brownian motion is statistically random and unbiased, an increase in the number of particles N results in a zero value of the second term in the right-hand side of Eq. (2). It means that the spatially averaged vector of the particle displacement (Fig. 6d) becomes equal to that of the fluid flow (Fig. 6e); it is therefore possible to reduce errors associated with Brownian motion and obtain accurate velocity vectors of the fluid flow while retaining temporal resolution. In brief, spatial averaging of particle vectors is carried out for each interrogation window using one pair of particle images. The time interval of the SAT–PTV system is the frame interval of the CCD camera (37 ms for C4880-80) for the present study.

3.3
Synthetic particle images for validation of SAT–PTV
To validate the capability of SAT–PTV for microspace velocity measurements, synthetic particle images considering Brownian motion of submicron tracer particles were generated by Monte Carlo simulation. Particles were randomly distributed in a three-dimensional velocity field with 256 grayscales. A spherical wave that goes through a circular hole from a point source of light creates the three-dimensional intensity distribution near the focal point. The scattering intensity and shape of defocused particles were calculated using the Lommel functions (Born and Wolf 1997). One example of images representing 400-nm diameter defocused particles is displayed in Fig. 7.

The mean square displacement of particle diffusion x_p associated with Brownian motion for the frame interval Δt is expressed as

$$\left\langle x_p^2 \right\rangle = 2D\Delta t, \qquad (3)$$

where the diffusion coefficient D is given by:

$$D = \frac{k_B T}{3\pi\mu d_p}. \qquad (4)$$

Here d_p is the particle diameter, k_B is Boltzmann's constant, T is the absolute temperature of the fluid, and μ is the dynamic viscosity of the fluid. The particle displacement resulting from Brownian motion was considered in the polar coordinate system. The magnitude of this

displacement was calculated by using the probability density function that is assumed to be a Gaussian distribution, which fulfills Eq. (3) (Einstein 1905), and the direction was randomly generated. Finally, the total particle displacement in the flow was represented as the summation of the fluid flow vector and that due to Brownian motion.

All the parameters in the present simulations were chosen to be the same as those for the reported experiments in this study: the dynamic viscosity of water is 854.4 µPa s at 293 K, the particle diameter is 400 nm, and the frame interval is 37 ms. Parameters used in Eq. (1) for the measurement depth are: n =1.515, λ =508, and NA =1.4.

Particle images in two types of flow fields, i.e., a uniform flow field and flow field with a linear gradient (Fig. 8), were generated. Three kinds of techniques, i.e., PIV, time-averaged PIV and SAT–PTV, were applied to measure velocity fields in the synthetic images, and the capability of SAT–PTV was examined in comparison with PIV and time-averaged PIV. The PIV technique in the present study is based upon a cross-correlation technique by Abe et al. (1998), and a Gaussian peak-fit method (Westerweel 1997) was employed to interpolate the sub-pixel displacement. Time-averaged PIV utilized ten ensemble-averaged instantaneous velocity fields.

3.4
Effect of the number of particles in the interrogation window
It is found from Eq. (2) that the accuracy of SAT–PTV depends on the number of averaged vectors, which means that an increase in the number of particles in the interrogation window yields high accuracy. Two methods to increase the number can be considered: (1) increasing the concentration of particles in the flow and (2) increasing the size of the interrogation window. For high particle seeding densities, i.e., when the former method is considered, it is difficult to track each particle, because the distance between particles is comparable to the mean displacement of Brownian motion within the frame interval for the present CCD camera used in this study. Therefore this section focuses on the latter method. The effect of the number of particles in the interrogation window on the measurement error of SAT–PTV in uniform flow (Fig. 8a), which was defined as the averaged difference between the known displacement and measured one, is investigated at a constant particle concentration of 1.11×10^{11} ml^{-1}.

Figure 9 shows profiles of measurement errors with increasing size of the interrogation window, i.e., increasing the number of 400-nm diameter particles in each interrogation window at the constant particle concentration. Results obtained by time-averaged PIV show smaller values compared to those by PIV and SAT–PTV, because time-averaged results contained ten instantaneous velocity fields. For example, when ten tracer particles exist in one interrogation window, time-averaged PIV uses 10×10 information. It is observed that the errors in SAT–PTV are suppressed in a whole range in comparison with those by PIV, especially when the number of particles was less than
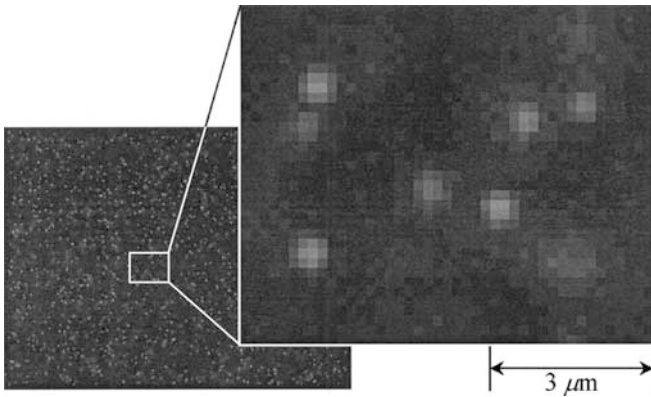
172

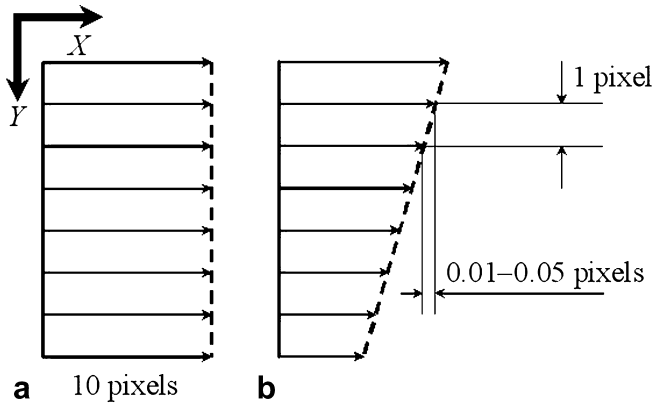
Fig. 7. Synthetic image containing 400-nm diameter particles

Fig. 10. Measurement error associated with velocity gradients measured by PIV, SAT–PTV and time-averaged PIV with the interrogation window of 40×40 pixels

Fig. 8. Schematic of **a** the uniform flow field and **b** flow field with the linear gradient in Monte Carlo simulation
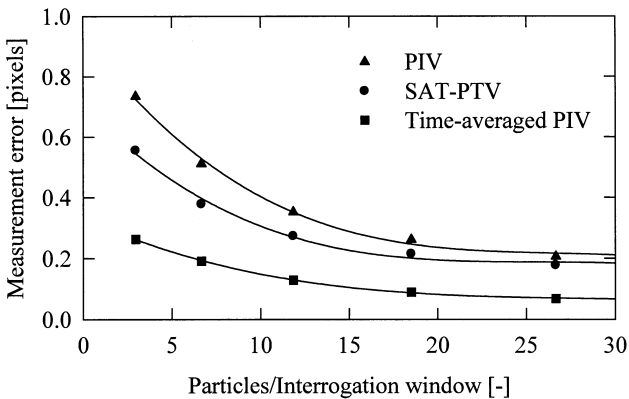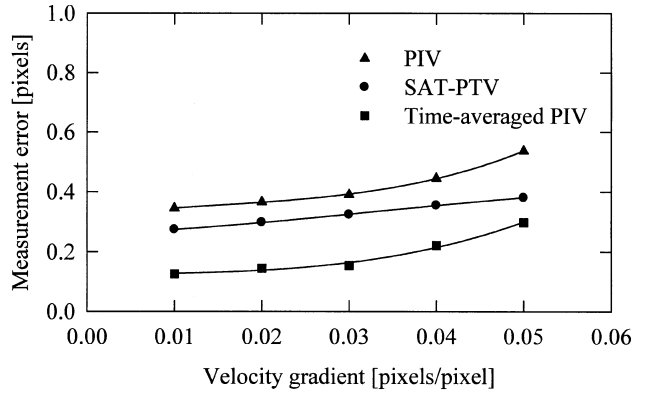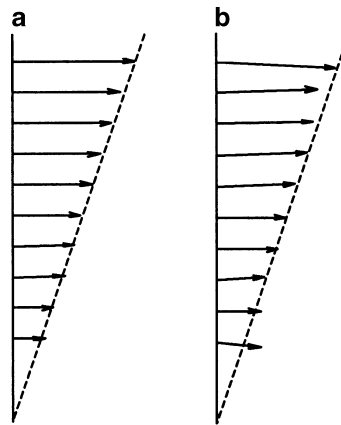

Fig. 11. Velocity profiles of the flow field with the linear velocity gradient of 0.05 pixels/pixel detected by **a** SAT–PTV and **b** PIV

Fig. 9. Measurement error associated with the number of tracer particles in the interrogation window measured by PIV, SAT–PTV and time-averaged PIV. Uniform flow was considered in the simulation

ten, SAT–PTV reduced the error of PIV by more than 20%. It means that by using SAT–PTV, it is possible to detect instantaneous velocity fields, thereby reducing the effect of Brownian motion. On the other hand, when the number of particles was over 25, the measurement error by PIV is nearly identical to that by SAT–PTV, because cross-correlation analysis using a large number of particles in

uniform flow was more successfully performed compared to the case of a few particles.

3.5
Effect of velocity gradients
Another important feature of SAT–PTV, its applicability to regions with velocity gradients, is examined with synthetic particle images (Fig. 8b). The size of the interrogation window was 40×40 pixels and 400-nm diameter particles were considered.

Figure 10 shows measurement errors with increasing magnitude of velocity gradient. Results obtained from time-averaged PIV show smaller errors, however, the significant increase in the error by time-averaged PIV, i.e., more than 100% increase at a velocity gradient of 0.05 compared to 0.01, as well as that by PIV is observed with increasing velocity gradient magnitudes. The effect of the change in the velocity gradient on the errors by SAT–PTV is small, i.e., less than 40% increase at a velocity gradient of 0.05 compared to 0.01. SAT–PTV is a robust method when the velocity gradient is unsteadily changed in microchannel flow, because SAT–PTV can track each tracer particle correctly. On the other hand, PIV contains the measurement errors, caused by spatial correlation with the interrogation window within which the velocity gradient is dominant.
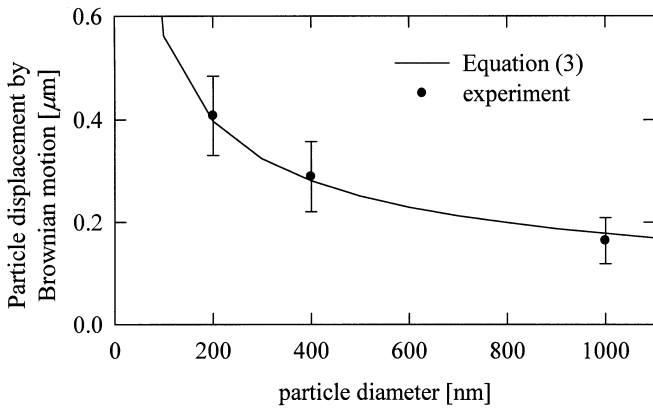
Fig. 12. Particle displacement by Brownian motion in the pressure-driven flow measured by SAT–PTV in comparison with the theoretical solution obtained by Eq. (3)
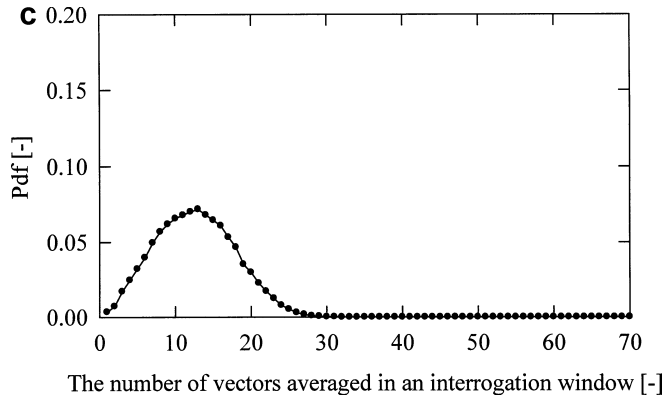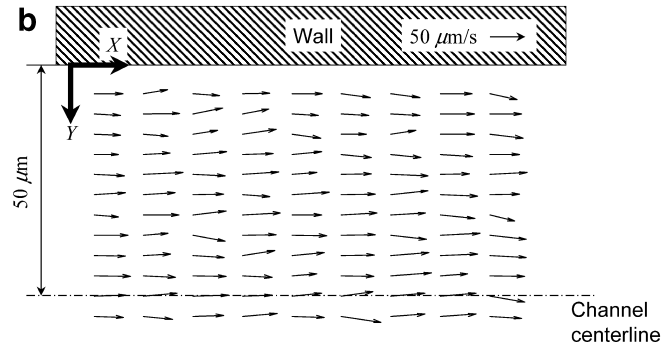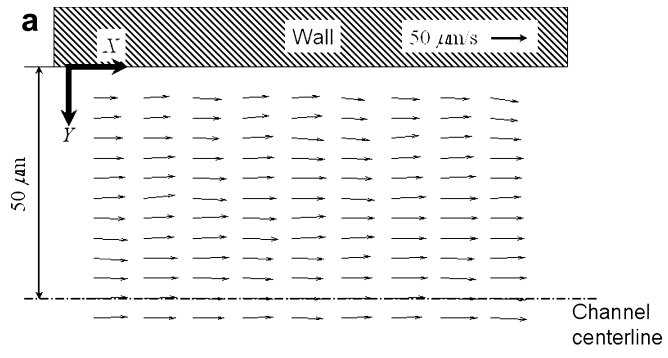

Fig. 13. Instantaneous velocity vector maps detected by a SAT–PTV, b PIV and c probability density distribution of the number of 400-nm diameter particle vectors in the interrogation window of 6.7 μm×6.7 μm (40×40 pixels)

Fig. 14. Instantaneous velocity vector maps detected by a SAT–PTV, b PIV and c probability density distribution of the number of 400-nm diameter particle vectors in the interrogation window of 10 μm×10 μm (60×60 pixels)
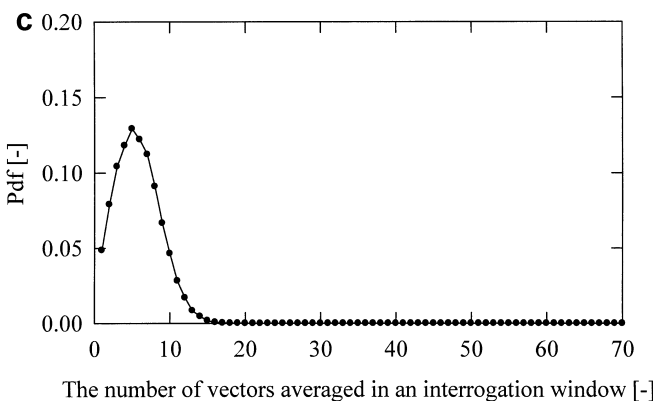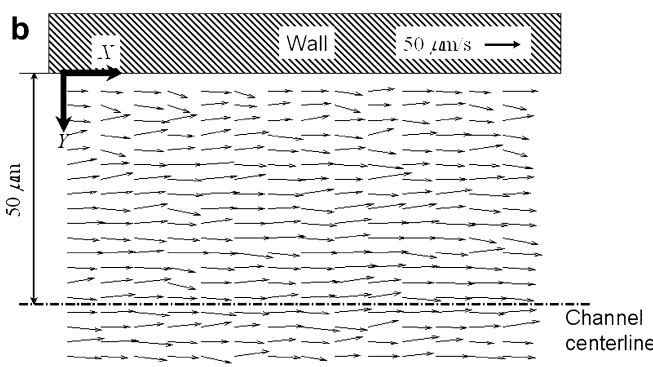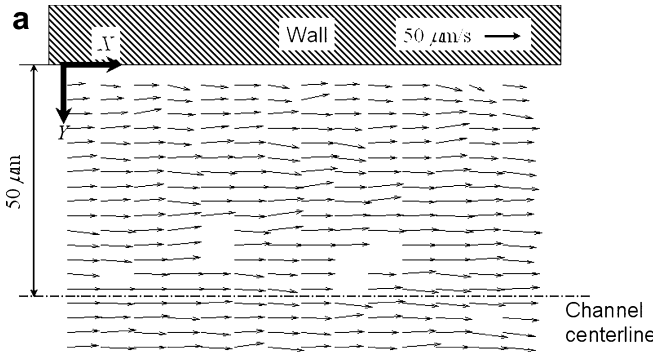
This result is confirmed by a velocity profile with a linear velocity gradient of 0.05 pixels/pixel detected by SAT–PTV in comparison with that by PIV (Fig. 11). It is observed that the SAT–PTV method can capture the velocity profile precisely, while PIV fails to detect the velocity profile. It can be concluded from validation using synthetic particle images that SAT–PTV can distinguish temporal variations of the flow with velocity gradients from velocity fluctuations associated with Brownian motion.

4
Results and discussion

4.1
Pressure-driven flow
The SAT–PTV method was applied to a pressure-driven flow driven by the height difference maintained between the inlet and outlet (Fig. 2). The Reynolds number was
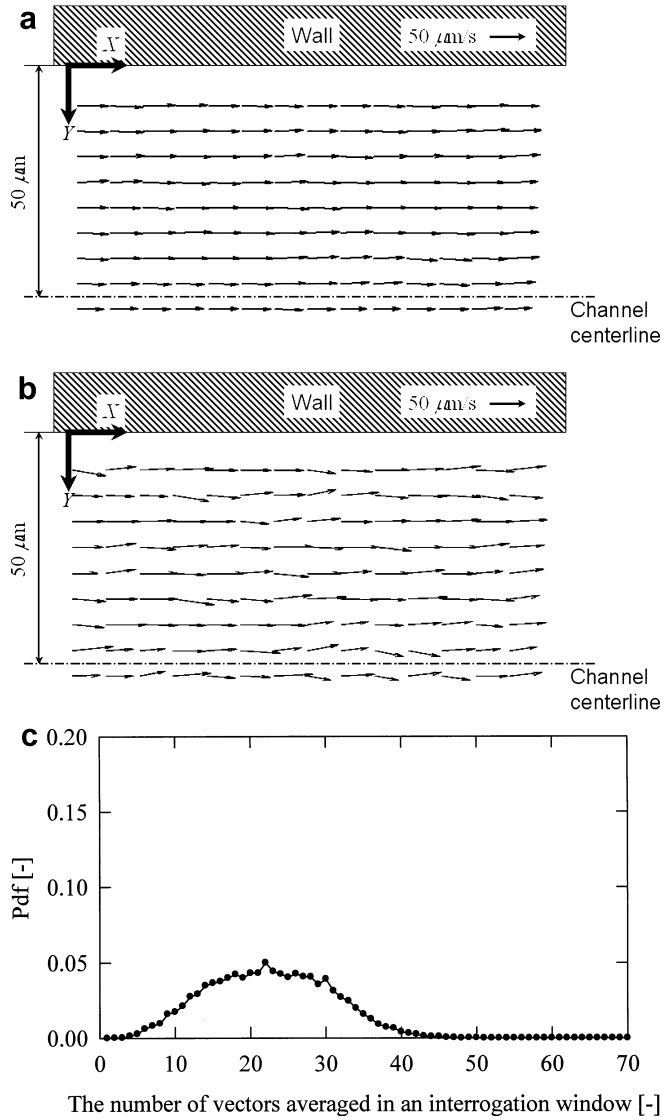
Fig. 15. Instantaneous velocity vector maps detected by **a** SAT–PTV, **b** PIV and **c** probability density distribution of the number of 400-nm diameter particle vectors in the interrogation window of 13.3 μm×13.3 μm (80×80 pixels)
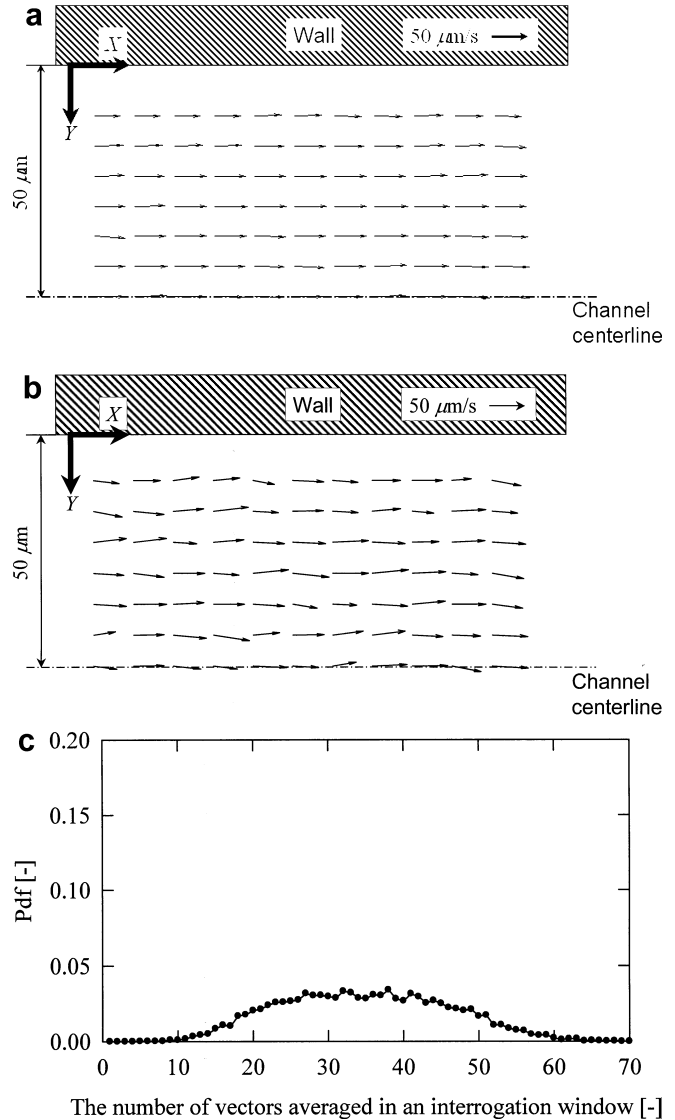

Fig. 16. Instantaneous velocity vector maps detected by **a** SAT–PTV, **b** PIV and **c** probability density distribution of the number of 400-nm diameter particle vectors in the interrogation window of 16.7 μm×16.7 μm (100×100 pixels)

$6.17×10^{-3}$. Three types of fluorescent particles were used, as listed in Table 1, to investigate the effectiveness of SAT–PTV in eliminating the effect of Brownian motion on velocity detection. The difference between the displacement of each particle and the mean displacement of particles in the interrogation window in the pressure-driven flow was measured by SAT–PTV and plotted against particle diameter in Fig. 12 in comparison with the particle displacement obtained by Eq. (3). Measurement results by SAT–PTV agree well with the theoretical solution, confirming that the particle displacement resulting from Brownian motion is eliminated by SAT–PTV, i.e., spatially averaged v_B in Fig. 6b goes to zero.

As SAT–PTV can reduce errors associated with Brownian motion by increasing the number of particles in the interrogation window, the size of the interrogation window was changed to confirm this conclusion obtained from Fig. 9. The size of the interrogation window was set at 6.7 μm×6.7 μm (40×40 pixels), 10 μm×10 μm

(60×60 pixels), 13.3 μm×13.3 μm (80×80 pixels) and 16.7 μm×16.7 μm (100×100 pixels), as shown in Figs. 13, 14, 15 and 16, respectively. In each figure, velocity vector maps obtained by SAT–PTV and PIV as well as the probability density distribution of the number of particle vectors in the interrogation window are exhibited. It is observed from Fig. 13 that even when the number of vectors was less than ten, SAT–PTV could capture the instantaneous velocity fields, despite the fact that pairing particles at two successive images was failed, which indicates the blanks in Fig. 13a. When the number of vectors averaged in the interrogation window was increased, i.e., a peak value of the probability density function was shifted to the right-hand side as shown in Figs. 13c, 14c, 15c and 16c, the instantaneous velocity vector maps detected by SAT–PTV showed a laminar flow pattern. On the other hand, velocity vectors measured by PIV are found in disorder, which is never neglected in spite of increasing the number of vectors.
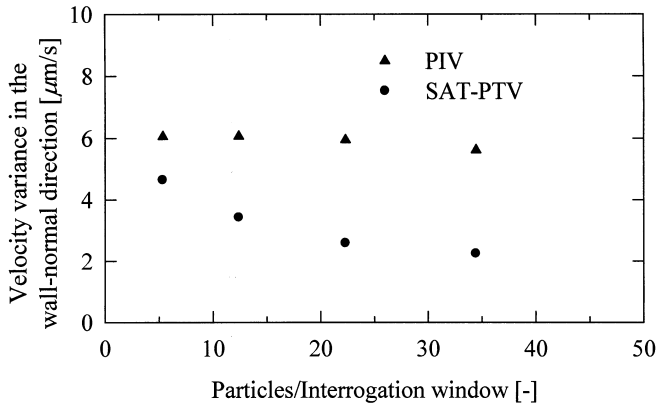
Fig. 17. Velocity variance in the wall-normal direction at the channel centerline against the number of tracer particles in the interrogation window, which was obtained from the experiments

For further insight into the effect of the number of particles on measurement results, velocity variance in the wall-normal or Y-direction at the channel centerline was plotted in Fig. 17 versus the number of particles in the interrogation window. It is obvious that the increase in the number of particles reduces velocity variances detected by SAT–PTV, which is consistent with simulation results in Fig. 9. The results by PIV indicate larger values even when the number of particles in the interrogation window was increased. This difference between SAT–PTV and PIV is confirmed by Fig. 10, in which PIV always contains the measurement error associated with Brownian motion in flow fields with velocity gradients.

It can be concluded from simulations and experiments that the increase in the number of vectors averaged in the interrogation window enables us to detect instantaneous velocity fields precisely, reducing the errors associated with Brownian motion. Therefore the present SAT–PTV method is more effective for less than ten vectors in the interrogation window without significant loss in spatial resolution.

4.2
Pulsating flow

A pulsating flow is considered in this section to confirm the performance of SAT–PTV for time-series measurements. Figure 18 illustrates a schematic of a microchannel with an electrokinetic pump operating at 5 Hz, which comprises two platinum electrodes sputtered on a cover glass slide. The applied electric field was 60 V/cm. The fabrication process is based upon a replica molding technique of poly(dimethylsiloxane) (PDMS) (Hosokawa and Maeda 2001). DI water seeded with 400-nm diameter fluorescent particles were injected at the inlet.

Figure 19 shows the temporal evolution of the velocity vector field detected by SAT–PTV. The size of the first interrogation window was 6.7 μm×6.7 μm (40×40 pixels) and approximately six vectors were averaged. It is observed from Fig. 19 that SAT–PTV captures the unsteady flow with temporal resolution of 37 ms, eliminating the effect of Brownian motion.

A power spectrum of velocity fluctuations normalized by the mean-squared velocity for the circle shown in Fig. 19 was plotted in Fig. 20 using fast Fourier transforms (FFT). The peak value corresponds to the frequency of the electrokinetic pump. SAT–PTV is confirmed to be a promising method to detect temporal variations of velocity fields in microspace.

5
Conclusions

A new method to measure velocity fields in microspace was developed to detect temporal velocity variations of the fluid flow considering Brownian motion of submicron tracer particles. The ability of SAT–PTV was examined using synthetic particle images calculated by Monte Carlo simulation. SAT–PTV was applied to pressure-driven flow and pulsating flow, in which micro-PIV cannot detect instantaneous velocity vector fields with temporal resolution. The important conclusions obtained from this work are summarized below.
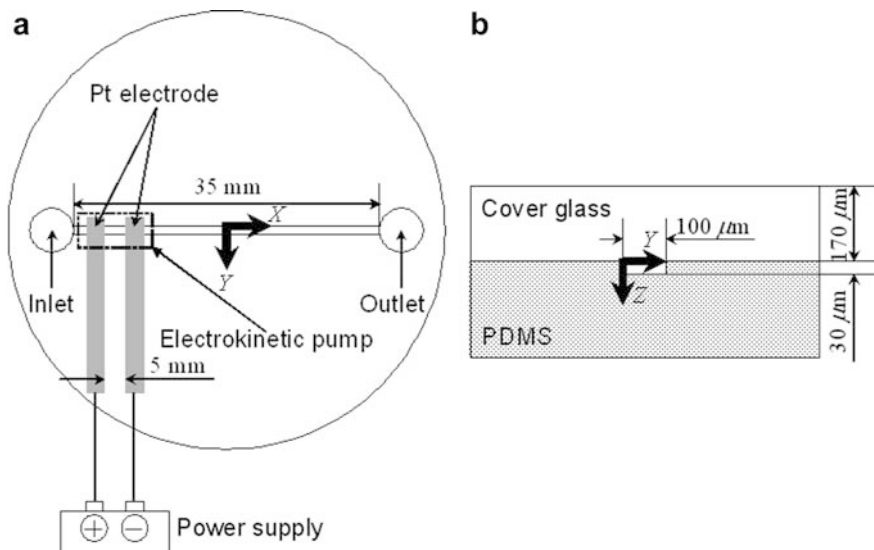
Fig. 18. a Top and **b** cross-sectional views of the microchannel with the electrokinetic pump

a $t = t_0$

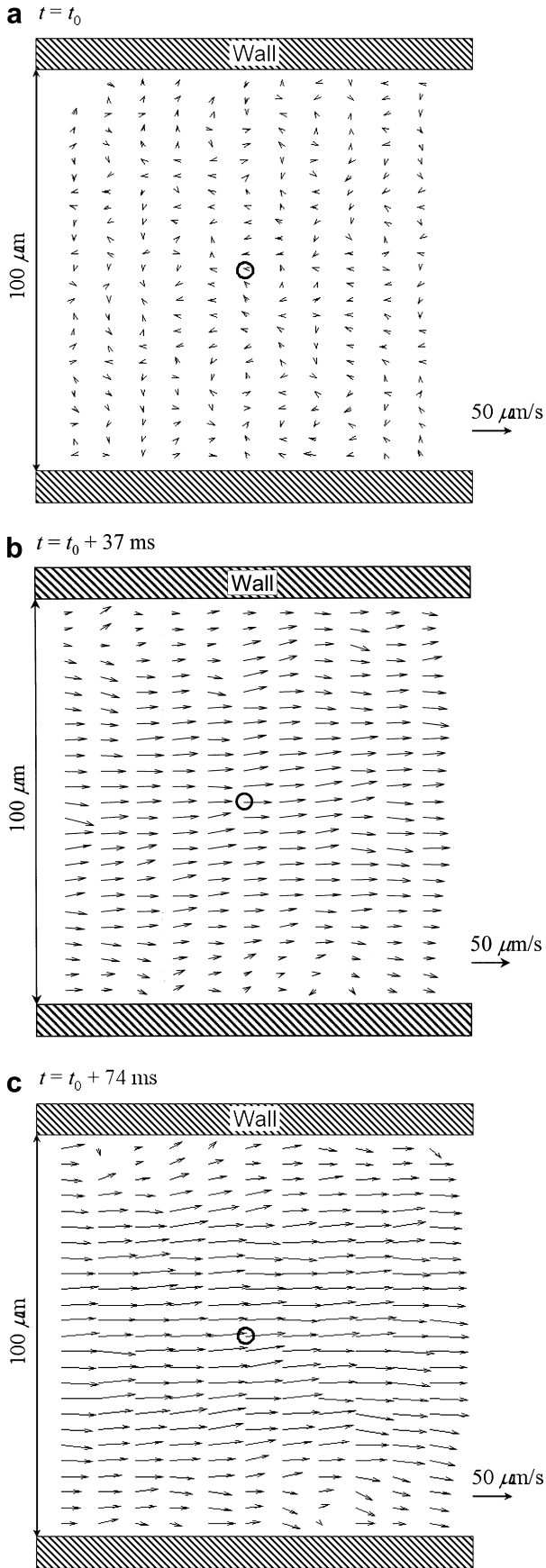**b** $t = t_0 + 37$ ms

c $t = t_0 + 74$ ms

◄

Fig. 19. Temporal evolution of velocity-vector field of the pulsating flow in the microchannel with the EK pump operating at 5 Hz, detected by the SAT–PTV method. The applied electric field was 60 V/cm. The time interval of each vector map was 37 ms. The *circle with the solid line* was used to calculate a power spectrum of velocity fluctuations as plotted in Fig. 20
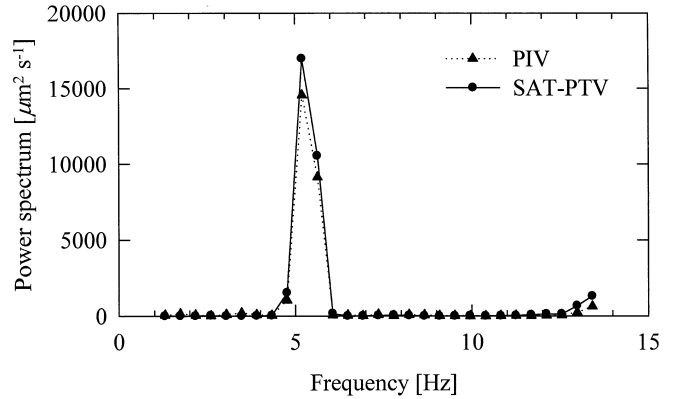

Fig. 20. Power spectrum of velocity fluctuations calculated at the *circle with the solid line* as shown in Fig. 19

1. SAT–PTV can eliminate the effect of Brownian motion on velocity detection with temporal resolution, spatially averaging PTV vectors within each interrogation window of PIV, since Brownian motion is spatially random and unbiased. This operation enables us to measure instantaneous velocity fields without losing temporal resolution.
2. The increase in the number of vectors averaged in the interrogation window reduced measurement errors of SAT–PTV, which was confirmed by simulations and experiments. The present method is more effective for less than ten vectors in the interrogation window without significant loss in spatial resolution.
3. Temporal variations of velocity fields in the pulsating flow were detected by SAT–PTV in time series, which cannot be measured by micro-PIV.

The temporal and spatial resolutions offered by SAT–PTV and PIV, respectively, are promising techniques to measure velocity fields in microspace for further development of microfluidic devices.

References

Abe M, Yoshida N, Hishida K, Maeda M (1998) Multilayer PIV technique with high power pulse laser diodes. In: Proc ninth int symp appl laser tech fluid mech (CD-ROM)

Adrian RJ (1991) Particle-imaging techniques for experimental fluid mechanics. Ann Rev Fluid Mech 23:261–304

Born M, Wolf E (1997) Principles of optics. Pergamon, Oxford

Brody JP, Yager P, Goldstein RE, Austin RH (1996) Biotechnology at low Reynolds numbers. Biophys J 71:3430–3441

Einstein A (1905) On the movement of small particles suspended in a stationary liquid demanded by the molecular-kinetic theory of heat. In: Theory of the Brownian movement. Dover, New York, pp 1–18

Hosokawa K, Maeda R (2001) In-line pressure monitoring for microfluidic devices using a deformable diffraction grating. In: Proc 14th IEEE int conf, pp 174–177

Keane RD, Adrian RJ, Zhang Y (1995) Super-resolution particle imaging velocimetry. Meas Sci Technol 6:754–768

Lanzillotto AM, Leu TS, Amabile M, Samtaney R, Wildes R (1997) A study of structure and motion in fluidic microsystems. AIAA paper 97–1790, 28th Fluid dynamics conf, Snowmass Village, CO, June 29–July 2

Meinhart CD, Wereley ST, Gray MHB (2000a) Volume illumination for two-dimensional particle image velocimetry. Meas Sci Technol 11:809–814

Meinhart CD, Wereley ST, Santiago JG (1999) PIV measurements of a microchannel flow. Exp Fluids 27:414–419

Meinhart CD, Wereley ST, Santiago JG (2000b) A PIV algorithm for estimating time-averaged velocity fields. J Fluids Eng 122:285–289

Santiago JG, Wereley ST, Meinhart CD, Beebe DJ, Adrian RJ (1998) A particle image velocimetry system for microfluidics. Exp Fluids 25:316–319

Sato Y, Irisawa G, Ishizuka M, Hishida K, Maeda M (2003) Visualization of convective mixing in microchannel by fluorescence imaging. Meas Sci Technol 14:114–121

Westerweel J (1997) Fundamentals of digital particle image velocimetry. Meas Sci Technol 8:1397–1392